A novel electroretinogram screening protocol can distinguish various mouse strains

Author: *BSc. Jochem Cornelis* (Student at the VU University, Amsterdam)
Written as final report for 2nd work placement for the Neuroscience Topmaster (VU/EUR) program
E-Mail / Student Number: pekel@dds.nl / 1154001
October 2007

Supervisor: Dr. J.A. Heimel[1]
Responsible lecturers: Prof. Dr. A.B. Smit[2] and Dr. C.N. Levelt[1]

[1)] Department of Molecular Visual Plasticity, Netherlands Institute of Neuroscience, Royal Netherlands Academy of Arts and Sciences, Amsterdam, the Netherlands.

[2)] Department of Molecular and Cellular Biology, Institute of Neurosciences, FALW, Free University, Amsterdam, the Netherlands.

Abstract

Introduction: The functioning of the retina is essential for human vision. Various genetic defects interfere with this, many of which remain to be identified. *Method:* We designed an electroretinogram (ERG) protocol to be used in forward genetic screens of mice. The protocol was designed to merely distinguish 'normal' and 'affected' strains and therefore it is sensitive to various aspects of retinal functioning at the same time. The protocol was tested on four inbred mouse strains: C57Bl/6J, DBA/2OlaHsd, C3H/HeNHsd (retinal degeneration – rd) and BALB/c (albino). *Results:* differences were identified between C57Bl/6J and all other strains. C3H mice did not show a response at all and DBA/2 and BALB/c showed a delayed a- and b-wave respectively. Parameters deduced from fitted Naka-Rushton like curves showed a different course of b-wave amplitudes over the range of flash intensities, for all groups. *Discussion:* The findings confirm that our protocol is suitable for the purpose of identifying strain differences. Subsequently this approach should be tested on mice that have the same genetic background except for one mutation.

Abbreviations

ERG – Electroretinogram

OP – Oscillatory potential (oscillations on the b-wave in the ERG)

STR – Scotopic threshold response

A-Wave – First negative going part of the ERG

B-Wave – Positive peak in the ERG

LED – Light emitting diode (for example, the power-on lights in electrical devices)

PWM – Pulse width modulation

Introduction

The visual system plays a vital role in most of our daily activities. Modern techniques may have improved the life of visually impaired, but when this system is partially or even fully affected, a patient is still presented with a serious handicap. The successful processing of visual signals depends on various subsystems, one of which is the eye, containing the retina where light is transformed into electrical signals.

Many visual diseases originate in the retina and genetic makeup often plays an important or even determining role in their emergence. The importance of mice in research concerning such diseases is twofold. First, identifying mice with visual impairments caused by genetic defects can often point to specific (human) genes that cause the defects.[2,3] And secondly, mice displaying symptoms comparable to those of humans (usually – but not necessarily – due to the same genetic defects as their human counterparts) can serve as mouse models.[4] Such models can give insight into the actual mechanisms between the genotype and phenotype, but they also provide opportunities to test out treatments.

Despite ongoing research linking genes to retinal impairment,[2,3,5-10] still many congenital factors remain unknown. Furthermore, a great deal of defects identified in humans remain to be translated into a mouse model.[3] An example is retinitis pigmentosa, which comes in different forms and is characterized by progressive loss of rods and cones. This causes disruption of night vision during adolescence, side vision in young adulthood and central vision later in life. Retinitis pigmentosa has a worldwide prevalence of 1 in 4000. Although 45 mutations already have been identified as risk-factors, still 60% of all patients have a genetic defect that remains as yet unidentified.[11]

If one wants to look beyond the most obvious candidates, forward genetic screens in mice can be used to search for mutations affecting the retina. Such a screen would require cheap and time efficient tests. To compromise, these tests merely need to divide the screened animals into two groups: normal versus affected. Different techniques can be used to make this distinction. These fall into three categories: morphological, functional and behavioral evaluation (reviewed by Pinto and Enroth-Cugell.[12] Although the latter is in many cases more time consuming and can suffer from interference of motor and learning deficits, all three complement each other. For example, in a screen on 9000 differently mutated mice, Pinto *et al.* used morphological as well as functional tests in search for abnormalities and found that the results only partially overlapped.[13]

A very suitable technique for functional screening of the retina in mice is electroretinography (ERG).[13,14] ERG recordings take only a short amount of time and can be obtained in vivo (under anaesthesia) in non-invasive matter in response to full field light stimuli.[†] The resulting signal represents the summed electrical activity of all cells in the retina. Depending on the conditions (stimulus, adaptation, background) ERG responses to single flashes of light show different components, of which the a-wave, b-wave and oscillatory potentials (OPs) are the most prominent.

The a-wave is negative going and emerges soon after stimulus onset. It is thought to originate in the photoreceptor cells.[13,15-19] The b-wave on the other hand is positive going, emerges somewhat later and is thought to be brought about by the bipolar cells[13,15,16,20] (connecting the granule and ganglion cell layers). On the positive slope of the b-wave, oscillations can be seen. Those are called OPs and are thought to be the result of interactions between bipolar, amacrine and ganglion cells.[16,21,22]

Many different problems can arise depending on the genetic makeup. For example, besides mice without any response at all, Pinto *et al.*, also found mice with slow a-waves or inverted/small b-waves. Other mice showed abnormalities in other components such as the scotopic threshold response (STR) and c-wave.[13] Some problems may only show up under certain conditions (e.g. adaptation level or stimulus type).[13]

Taken together, this suggests a whole battery of tests to find all possible abnormalities. This increases the duration and feasibility of the experiments, which is highly unwanted since the throughput rate is essential for screening.

Based on the assumption that we only need to discern between two groups of genotypes ('normal' and 'affected'), we propose a short protocol that incorporates many different aspects of the ERG signal. We measured ERG signals from mice of four strains: C57Bl/6J, DBA/2OlaHsd, C3H/HeNHsd and BALB/c to see whether our protocol could detect any differences.

While C57Bl/6J mice can be thought of having 'normal' vision, C3H mice show profound abnormalities. In these mice, severe retinal degeneration emerges already a few weeks postnatal: morphogenesis in the photoreceptor cell layer is disordered, which eventually leads to cell death.[23,24] BALB/c mice are albino and show a more severe progress of photoreceptor degeneration

[†] As a matter of fact, ERGs can also be recorded in reaction to more complex stimuli, this is called 'pattern ERG' and falls beyond the scope of the current research.

than C57Bl/6J mice do, although this does only become apparent after 8 months.[25] Albino mice however lack pigment in the retina and show behavioral difference associated with photophobia: 8 weeks postnatally they show less open-field activity than pigmented controls but only under bright light.[26] DBA/2 mice develop glaucoma. This does not set in before 6-12 months postnatally and is characterized by an elevated intraocular pressure (IOP), axonal degeneration in the optic nerve and apoptosis of retinal ganglion cells.[27] Previous ERG experiments however suggest subtle differences between DBA/2 and C56Bl/6J already at 6 weeks of age[14].

We have compared the aforementioned strains at 6 weeks of age and conclude the proposed protocol is sensitive enough to pick up various strain differences fast and effectively.

Results

ERG responses to 10 flash stimuli of different insentity (measured in cd*s/m^2) were recorded. Each flash was presented 30 times and responses were averaged. Such a 'run' was done two times consecutively per mice. Figure 1 shows typical ERG responses from one run from one mouse (30 sample averages). For C3H the response seems zero and both BALB/c and DBA/2 appear different from the C57Bl/6J. To distinguish true differences from normal variation quantification is needed.

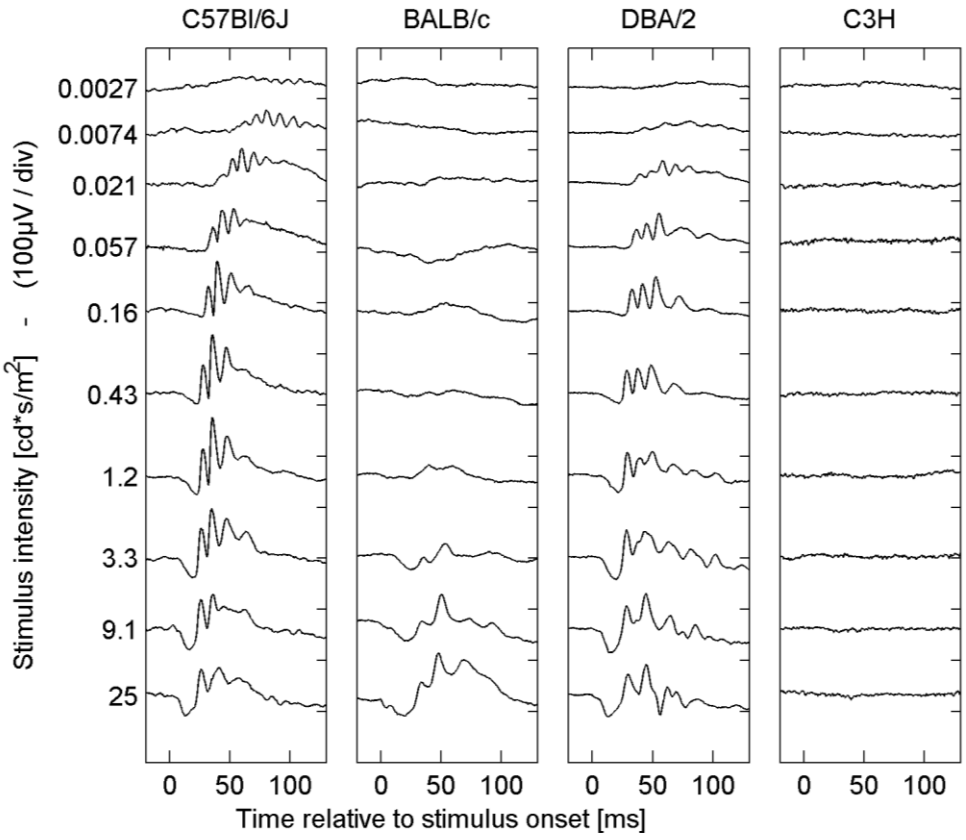

Figure 1. Typical ERG responses to single flashes at time 0, for all 4 mouse strains. Responses are 30 sample averages of one mouse.

Therefore we compared the strains on different properties of their ERG waves: a- and b-wave amplitude and implicit times (see figure 2), for the 25 cd*s/m^2 flash.

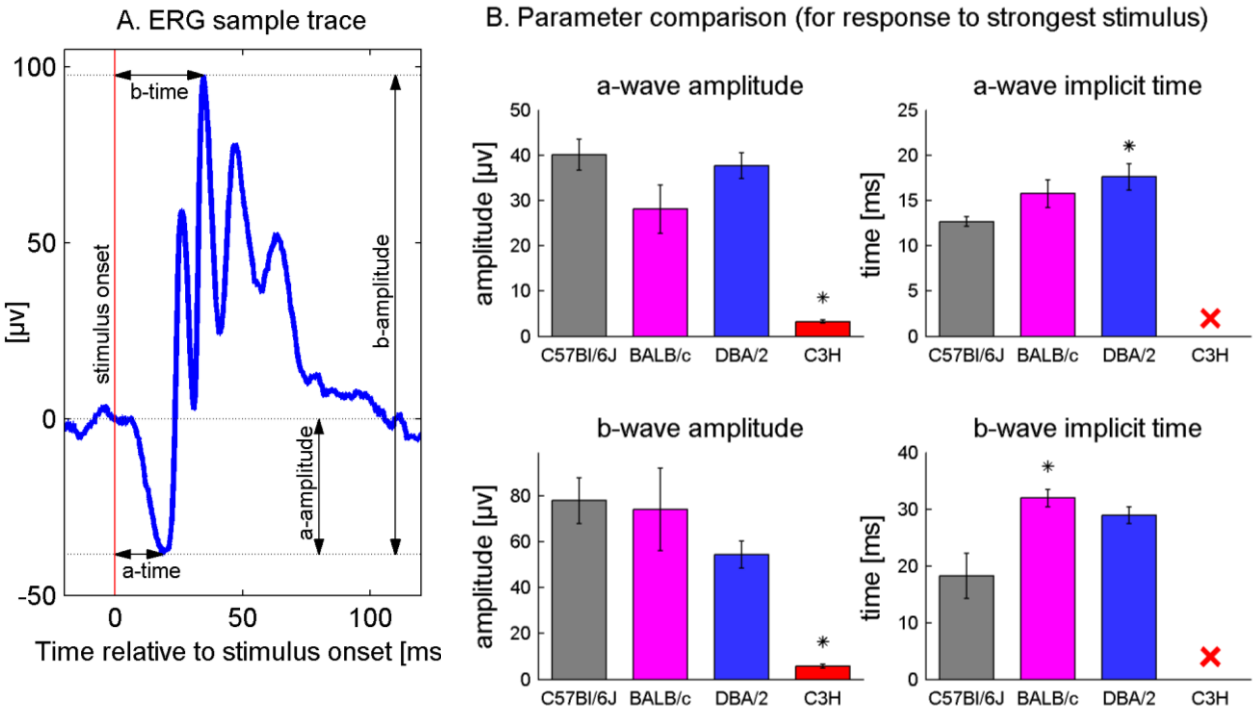

Figure 2. A comparison of the four inbred strains on a- and b-wave amplitude and time. **A)** 30-sample average ERG response showing typical a-wave, b-wave and oscillatory potentials. Implicit times are measured with respect to the stimulus onset. The a-wave amplitude is defined as a-trough to baseline and the b-wave amplitude as a-trough to b-peak. **B)** Bar-plots with SEM of a- and b-wave amplitude and implicit time of responses to one stimulus (25 cd*s/m^2). Statistics are based on data per mouse (each data point is the average of the two runs within one mouse). A * indicates a significant difference ($p < .05$) with C57Bl/6J. *Note:* C3H times are irrelevant: the location of peaks and troughs was highly or fully subject to noise. *N* is 4, 3, 4 and 2 for the four strains respectively.

The C3H mice did not show any response at all. This was significantly different from the C57Bl/6J group for both a-wave ($t(3.1) = -12.6$, $p < .001$) and b-wave ($t(3.0) = 7.3$, $p = .005$). Explicit times (the time between stimulus onset and a- or b-point) could not be analyzed because the amplitudes did not rise above noise level.

For the implicit times, DBA/2 showed a moderately significant difference from C56Bl/6J, $t(3.8) = -3.17$, $p = .036$ on a-wave implicit time and BALB/c on b-wave implicit time, $t(3.9) = -3.2$, $p = .034$. Given the fact we have a low *n,* only moderate significance levels and are performing multiple tests, these data should be interpreted with caution.

A more pressing problem here is that we incorporate only a small fraction of our data. But the graphs in figure 1 suggest that some strain differences might be seen only at certain intensity

levels. Dalke *et al.* used a similar stimulus protocol and analyzed responses to 2 flash intensities.[14] This can still mask many differences but increasing the number any further, whilst maintaining a point-by-point comparison approach would make it hard to interpret the data.

To investigate the course of the b-wave amplitudes as intensity increases, we fitted a modified Naka-Rushton curve on the b-wave amplitude points as a function of stimulus intensity. We did this for each experiment 'run' (see figure 3A). From these fit functions two parameters were deduced: maximum response and log-i50 – the log10 of the intensity where the response is at 50% of the maximum response (see figure 3B).

When the aforementioned parameters are plotted against each other (Figure 3C) it appears that the groups occupy relatively separate areas of the plot. To quantify this we compared the groups on each of the two parameters separately (figure 3D). Compared to C57Bl/6J, the BALB/c mice showed a significantly lower log-i50 value: $t(2.3) = -10.8$, $p = .005$ and the DBA/2 mice showed a significantly lower maximum response: $t(4.1) = 3.4$, $p = .027$.

Finally, we also analyzed the oscillatory potentials – OPs (figure 4A). These oscillations – seen mostly on the rising edge of the b-wave – are thought to be one of the most sensitive parts of the ERG,[28,29] but sadly analyzing them is less straightforward.[21] Therefore, we only analyzed the frequency spectrum (figure 4B). Both rod and cone activity contribute to this spectrum, but rod activity centers around 110Hz, while cone activity shows a peak at 65Hz.[30,31] We calculated the ratio between the spectrum power at both frequencies (figure 4C). Although the resulting ratios fluctuate a lot over stimulus intensities, the plot roughly shows that 110Hz levels are higher in the beginning for low intensities (ratio > 1) but that the opposite is seen in response to stronger flashes. Groups were finally compared by the ratios at the highest flash intensity (figure 4D) showing the BALB/c had a lower ratio: $t(3.5) = 3.9$, $p = .02$.

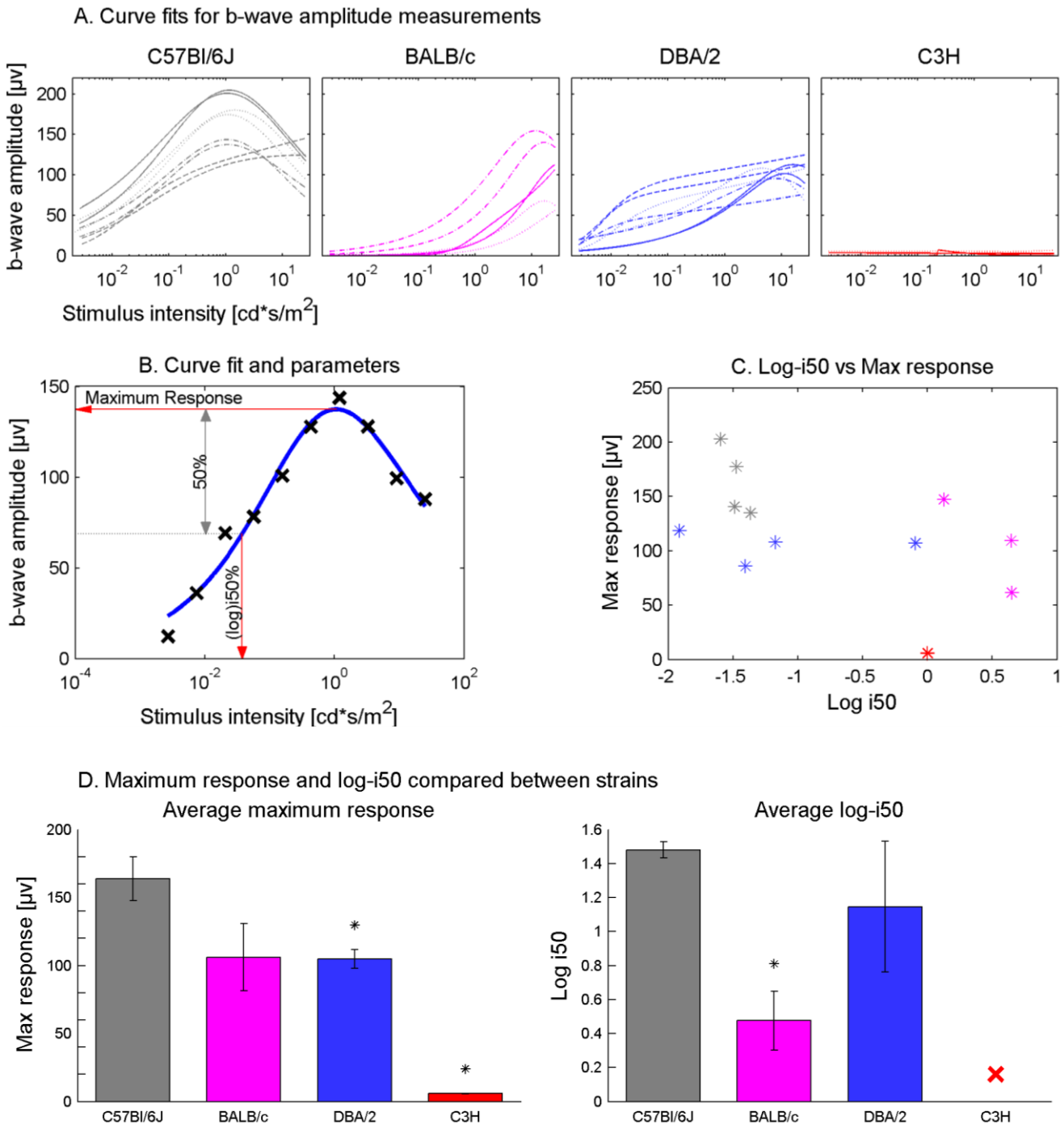

Figure 3. Parameters derived from fitted Naka-Rushton curves show differences in the course of b-wave amplitudes. **A)** Curve fits for b-wave amplitudes. Lines within one graph that have the same style are from the same mouse/experiment. **B)** Typical fitted curve. The markers show the actual responses. Arrows indicate how the two parameters 'maximum response' and log-i50 were derived. **C)** 'Maximum response' versus the 'log10 of the intensity where the response was 50% of the maximum'. Each mark represents the average of the data from two 'runs' within one mouse. **D)** Bar plots with SEM for each of the two parameters, * indicates a significant difference ($p < .05$) with C57Bl/6J. Since the response in the C3H group did not exceed noise levels, the log-i50 values were not interpretable (for figure C this value was fixed at 0 for this group). *N* is 4, 3, 4 and 2 for all four strains respectively.

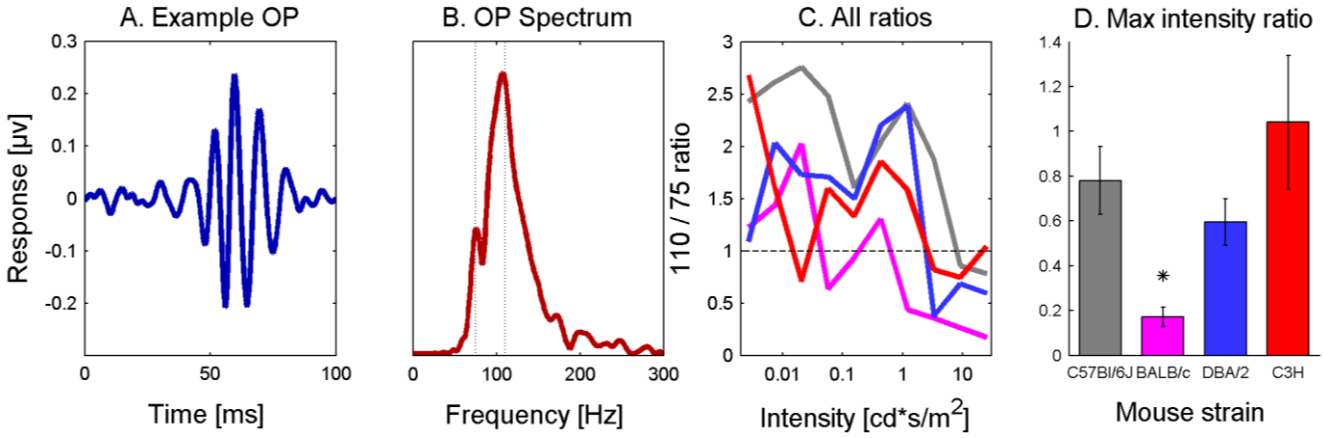

Figure 4. In OP spectra of responses to the low intensity flashes the 110Hz component is more prominent than the 75Hz. **A)** Typical OP waveform (30-sample average, 65-300Hz bandpass filtered). **B)** Single-sided frequency spectrum of the OP waveform in plot A. **C)** Ratios between spectrum power at 110Hz and 75Hz, each line represents one inbred strain (for explanation of colors see D). **D)** Bar-plots with SEM for the 110/75 ratios of the OP response to the strongest stimulus (25 cd*s/m^2). Statistics are based on data per mouse (each data point is the average of the two runs within one mouse). *N* is 4, 3, 4 and 2 for the four strains respectively.

Discussion

We have shown that our approach is suitable to discern different mouse strains. Not only did all tested strains differ from C57Bl/6J, they also did so differently. This means they can be discerned from each other as well. By deliberately choosing a stimulus protocol that does the opposite of isolating individual features, we were able to keep the duration of the experiments short, although we sacrificed the possibility to explain the origin of the differences. Once a mutant has been identified, questions about the underlying mechanisms should be addressed using protocols that are more specific.

Are our findings in agreement with previous results? For the **C57Bl/6J** some differences can be mentioned, although they are most likely caused by differences in the stimulation protocol. First, the overall signal was noticeably different from other light-adapted measurements, especially the presence of a clear a-wave was not seen in previous experiments. In fact, the signal showed more resemblance to the dark-adapted ERGs. This is probably due to the fact we do not use a background light between flashes. Second, our b-wave amplitudes showed super-saturation: at the highest intensity flashes the signal dropped again. Although this can be seen in humans and is called ‘photopic hill’, this phenomenon is not present in mice. In our case it is more likely this effect is caused by the relatively short periods between flashes.

It is widely known that the different **DBA/2** mice strains show problems in morphology, behavior and electrophysiology, due to glaucoma. However, these symptoms emerge only after 4-8 months of age.[27,32,33] Dalke *et al*. did find some differences between DBA/2NCrlBR and C57BL/6JIco mice: at the two flash intensities presented the DBA/2NCrlBR appeared to have a lower b-wave amplitude, although the results were not significant.[14] When comparing amplitudes (see figure 2) our data showed just that, but after incorporating responses to all the intensities we did notice a significant decrease (see figure 3). Although this suggests our method is more effective, the result could also be caused by differences in the various DBA/2 subtypes.

C3H mice carry the rd gene[34] and a few weeks postnatal, retinal degeneration already sets in. In our ERG experiments, these mice did not give a noticeable response by visual inspection of the signal. Although quantification appears to show some remaining signal, even after noise correction (see methods), this is not distinguishable from noise since the time of the a- and b-points appeared to be random. These findings are in line with the morphology of severe retinal degeneration[23,24] and behavioral research showing 8 week old C3H/HeJ mice to perform at chance level.[35] Dalke *et al.* did see discernable a- and b-waves in some C3HeB/FeJ mice, although they were very small and maybe not picked up by our approach due to slightly higher noise levels.

BALB/c mice are albino and lack pigment in the retina. Wong and Brown found BALB/cJ mice to perform worse than C57Bl/6J mice in visual learning tasks, but this difference could also be attributed to differences in learning capacities.[35] In a study by Bravo-Nuevo *et al*. young (P100) C57Bl/6J mice showed a significantly higher b-wave amplitude than BALB/cJ mice.[36] Pigmented mice also showed shorter implicit times. Except for the fact that their mice were older (P100 vs P42 in our experiments), these findings are in agreement with our results. Another possibility of the observed differences could be that dark adaptation in albino rodents is slower,[9,21] causing them to benefit less from the relatively short periods in the dark during the experiments compared to pigmented mice. That would be in agreement with the 110/75Hz ratios (see figure 4-C and D), which also suggest less rod activity (and thus less dark adaptation). This remains speculation however since our approach is only designed to pinpoint differences, not to explain them.

Even though we have shown our approach to be effective in finding strain differences, there might still be aspects of the ERG that we have missed, aspects that in other cases could be the only difference between two strains. First, mice have cones containing an UV pigment that does not get excited by the light stimulus used in our experiments. There is a evidence showing co-expression of

both UV and 'normal' non-UV (M) pigments,[37,38] suggesting this issue would be less relevant since our LED would in that case at least stimulate all cones. On the other hand, some cones seem to be pure-UV and thus the overlap appears to be partial,[39] showing a gradient from pure M cones in the far dorsal regions of the retina, via cones co-expressing M and UV pigments, to pure UV cones in the far ventral regions.[37-41]

Second, one can doubt whether our protocol actually elicited any rod response at all. Animals were tested in the day-time period of their diurnal rhythm and not dark-adapted before the experiments. On the other hand is it highly unthinkable that rods play no role at all, especially since the period between flashes is spent in the dark. The shape of the responses endorse this: a-waves - typically attributed to rod activity[6,8,13] - were clearly distinguishable. Furthermore, the 110Hz/75Hz ratio of the frequency spectrum was clearly above 1, while pure cone responses show a peak at 75Hz resulting in a ratio < 1.[30,31] Definitive conclusions however should only be drawn after testing a pure-rod mouse model.[8]

Third, more deficits could perhaps be brought to light by additional approaches, such as flicker/sinusoidal stimulations,[28,42-47] spectral sensitivity,[39] STR and c-wave analysis,[13] or substance administration.[48] Every expansion of the protocol however would complicate and prolong the experiments, putting stress on the throughput rate.

In the end, the essence of our approach might also turn against us. A protocol sensitive to different abnormalities is also subject to various sources of 'normal' variation. This variation may occlude smaller effects. The current results suggest this variation is surmountable but concerns relatively diverged strains. More definite conclusions can be drawn when the protocol is used to discriminate mutants from animals with the same genetic background.

Methods

Animals

Male mice from four different strains were ordered from Harlan Netherlands B.V.: C57Bl/6J, DBA/2OlaHsd, C3H/HeNHsd and BALB/c. This was organized in such a way that mice were around 6 weeks of age at the time of the experiments. This was in line with the approach of Dalke *et al.*[14] and is very close to the age at which ERG signals were found to be maximal[14,49]. During the period between arrival and experiments mice were kept in a local animal facility with a 12h dark/12h light cycle.

The experiments were done in compliance with guidelines provided by the Royal Dutch Academy of Sciences and carried out with permission of the Academy's animal experiment committee.

Apparatus - Recording

The ERG was recorded from the cornea with the other eye (closed) serving as a reference[13]. An electrode on the back served as ground signal. Ag/AgCl electrodes (obtained by chloriding a silver wire in common household bleach) were used. The signal was amplified using a differential amplifier (Model 1700 differential A-C amplifier; A-M Systems; amplified 10^4 times and filtered using a 1-1000Hz band pass filter). A PC equipped with a dedicated IO board (NI-DAQmx PCI-6229, National Instruments) was used for DA conversion (10Khz sampling rate; 320µV resolution), storage and off-line analysis.

Apparatus – Stimulus presentation

Figure 5. Stimulator and ganz-feld sphere.

To present the mouse with homogeneous stimuli of a broad (4 orders of magnitude) range of intensities, a custom developed system was used. Part of this system contains a Styrofoam sphere. The mouse's head is placed in the middle of this sphere and light is projected from underneath the mouse into the sphere (see figure 5). This way, direct light could reach its retina, while the indirect reflections from the Styrofoam provided ganzfeld stimulation.

A super bright blue LED was used to create the light pulses (Luxeon V Royal Blue; LXHL-PR02, 455nm – see figure 6 for typical spectrum, Philips Lumileds Lighting Company). To create such a wide luminance range of stimuli, three modifications were combined. First, pulse with modulation (PWM) with a carrier frequency around 22.8kHz (which is much faster than the typical timescale of the mouse retina[50]) was used to modulate the pulses between 10 and 100%. Furthermore, the duration of the pulse was varied between 0.5 and 5 milliseconds, which is still short enough to be integrated and perceived as a single pulse.[50] Finally, the system could switch between two LED currents: the maximum of 700 mA and 1/100th of that.

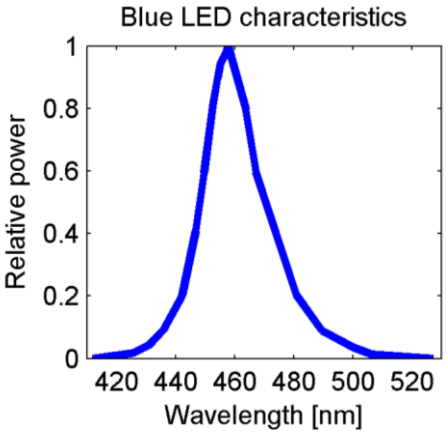

Figure 6. Blue LED emission spectrum.[1]

Before every experiment, the system was calibrated using a photodiode in a controlled position (at the end of the sled, where the mouse head would normally be positioned). The photodiode was attached to an integrating device that could be synchronized with the light pulses using an external trigger. This device eventually presented a digital signal based on the total amount of light that was collected by the photodiode during the whole pulse. This signal was used as a constant reference for the calibration.

To confirm that the mouse indeed responded only to the total amount of light presented during the pulse duration and nothing more, we designed three 'equal' stimuli based on different combinations of characteristics (pulse height, width or total duration). These three stimuli were in fact expected to have the same effect on the ERG, since in total the amount of light presented was equal for each of them. Figure 7 shows the results for one mouse. The observed variation is small but the pattern was comparable over all experiments, suggesting a small but 'real' effect. Since this difference is small and only involves the peak latencies, while the main focus of our analysis was on amplitude, the differences were taken for granted.

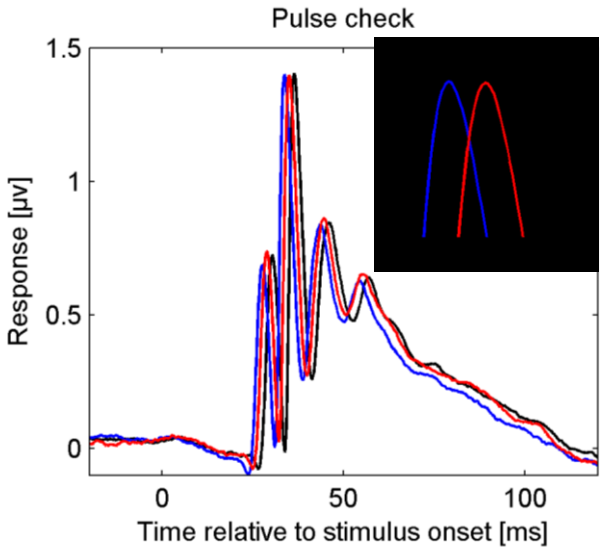

Figure 7. Response of three different stimulus types that contained the same amount of light. 90 sample averages. Pulse configuration (duration / height / 22.8kHz pulse width): blue = 0.5ms / high / mediocre, red = 2.5ms / low / mediocre, black = 5ms / low / small. *Inset*: magnification of the graph peaks.

Interestingly, this latency followed the pulse duration qualitatively but not quantitatively: longer pulses resulted in higher latencies, but the difference in time between the response peaks (2.5ms) was lower than that between the stimulus durations (4.5ms).

We wanted to be able to compare the intensities of our stimuli with those of other research groups. Because we use non standard colored light source we could not use radiance (which is based on Watts) for this. We needed a measure

that took into account the relative sensitivity of the mouse eye (for the light spectrum). Luckily, for the lower wavelengths (the only wavelength present in our and other's stimuli) the mouse's sensitivity function is very comparable to that of human scotopic (night) vision.[37,48] This enabled us to use scotopic candela (cd) measure for the comparison.

To get from the photodiode readout to the candela value, we assumed the LED and photodiode characteristics remained constant over intensities and time. The photodiode readout was first converted to watts based on calibration values using a photometer and linear interpolation between the calibration points. Subsequently, we corrected for the mouse eye relative sensitivity (to the LED frequency spectrum, which was derived from its specifications). The mouse eye relative sensitivity curve was set to 1 at 555nm and this is known to correspond to 638 lumen/watts.

Preparations

Experiments took place during the morning, starting approximately 3 hours after the light in the facilities had switched on. By starting each experiment roughly at the same time (with respect to the local light regime) we eliminated any risk of variation due to diurnal rhythm and prior light/dark rhythms.[51] All preparations were conducted under room light conditions.

Mice were anaesthetized with urethane (Sigma, The Netherlands). The injection was placed intraperitoneal and the dose depended on bodyweight (2 g / kg for C57Bl/6J and 2.2 g / kg for the other strains based on previous experience, 10% solution in saline). The disadvantage of urethane is that it is carcinogenic and can only be used for acute experiments. Conversely, it has a very prolonged effect compared for instance to ketamine/xalazyne solutions: only one injection is enough to keep the animal anaesthetized for over 8 hours. Furthermore our lab has a lot of experience with this anesthetic and the acute aspect of the experiments prevents any stress mice normally encounter while recovering from anesthesia. The depth of anaesthesia was ascertained by assessing the interdigital pinch withdrawal reflex.

Next, a subcutaneous injection of atropine sulphate (0.05 mg / mL in saline, 0.1 mg / kg bodyweight) was administered to reduce mucus production and thus minimize breathing problems.

Once anaesthetized, the mouse was transferred to a heating blanket as quickly as possible (Homeothermic Blanket Control Unit, Harvard Apparatus). Using feedback from a rectal temperature probe, body temperature was kept at around 36.8°C. A constant temperature was not

only important for the stability of the mouse, but also for that of the ERG signal, since it was found to be affected by body temperature.[52] From this point onward, the mouse was placed with its front teeth hanging over a bite-bar and some extra oxygen was provided using a small tube with its opening close to the mouse's nose.

Subsequently, one of the eyes (the one that would serve as a reference) was closed and prevented from re-opening with a single suture through the upper and lower eyelid. To also prevent light from reaching the retina of this eye by passing *through* the skin, it was covered with small pieces of black adhesive tape. The effectiveness of these measures were checked every time, the procedures of which are discussed in the protocol section.

Electrodes were attached in different positions. The reference electrode was gently hooked in a corner of the eyelid before covering it with tape while the measurement electrode was brought into contact with the upper part of the open eye's cornea. A third electrode, applied subcutaneously not far behind the head, served as ground.

When the mouse was properly prepared and recording signals looked alright, a single drop of atropine sulphate (0.05 mg / mL in saline) was released on the measurement eye to assure pupil dilation. Immediately after applying the atropine the sled was shoved into its holder. This way the mouse's head became situated inside the Styrofoam sphere. The final location of the sled, as well as the location of the bite-bar and therefore the mouse's head was always kept the same.

The mouse was subsequently placed in the dark by covering up the entire setup. Although a first protocol run was initiated immediately hereafter, this data was discarded to eliminate variation right after atropine administration. This would take around 10 minutes and the real experiments would be started directly after.

Protocol

Assuring the reference eye is closed

To assure the reference eye did not give any visual response, the reference electrode was disconnected from the amplifier and the input from the ground electrode was connected instead. Since this electrode was already used as ground signal to the amplifier, the reference part of the signal would always be 0, in fact taking away the differential nature of the amplification. Therefore, the resulting signal (reference eye with respect to the ground electrode) was contaminated with

noise and biological artifacts such as cardiac rhythm. To be able to still distinguish the ERG signal, 100 repeated measures (flashes of 25 cd*s/m^2, 700 ms apart) were taken and averaged. This way we were able to assess the effectiveness of the eye-cover without the need for more electrodes. Figure 8 shows typical responses from correctly (A) and partially (B) closed eyes. The latter shows how important this test was, because even an eye that on visual inspection seemed to be closed and covered successfully (with a suture and tape respectively) could still give a response such as seen in figure 8B. Figure 8C gives an example of how the signal would look like when measuring the *measurement eye* with respect to ground without subtracting the reference signal (in this case the reference eye input to the amplifier was replaced by the ground electrode signal).

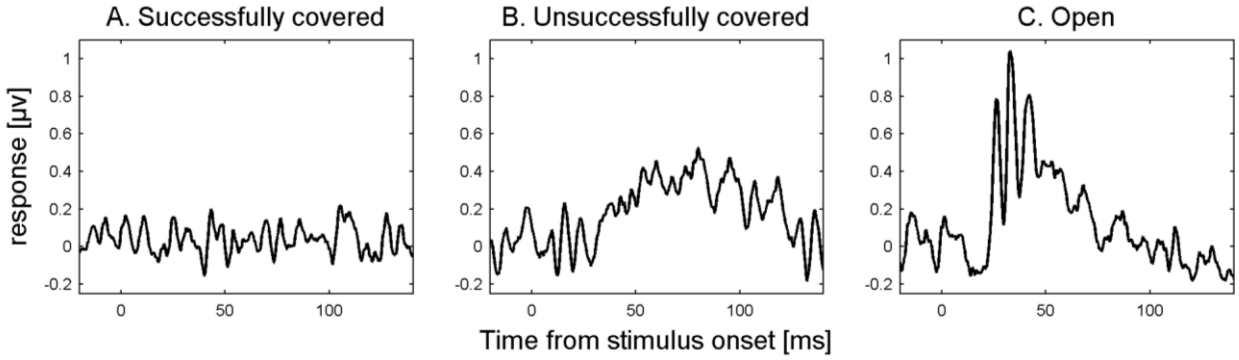

Figure 8. The effectiveness of the cover is assessed by inspection of a 100 sample average of non-differentially amplified responses of one eye. **A)** The response from a successfully closed/covered eye. **B)** A typical response of an eye that could still see despite of the suture and tape. **C)** A typical response of a fully open eye.

Stimulation protocol

The ERG was measured in response to light pulses of increasing intensity (0.0027 to 25cd, logarithmically spread over 10 levels). Each intensity was repeated 30 times. Pulse lengths ranged from .5 to 5 msec. Between pulses there was a delay of approximately 2 seconds (.5Hz). No *extra* delay was introduced for the transition from one intensity level to the next. Between pulses, no background lighting was present.

A delay of 2 seconds is too short[50] for a full recovery from the highest intensity pulses, causing differences between strains to show up as soon as their recovery speeds differ. Furthermore, the lack of preceding dark adaptation as well as background lights during the experiments results in a mix between photopic and scotopic ERG characteristics. Together, a number of qualities of the ERG and possible underlying biological cause could influence the results, which was exactly our aim.

Analysis

Outlier detection and sample averaging

Before averaging, the 30 samples were subjected to an automated outlier detection algorithm. Effectively, this algorithm removed those samples that affected the group mean disproportionately compared to the others (eg the samples that were too divergent to be masked by the sample averaging). For each sample we calculated how much the root mean square of the group-mean signal would change if that sample was to be removed. Every sample that had a bigger effect than a certain threshold was thrown away. This threshold was defined as: the median effect *plus* three times the smallest effect. In most cases none or only one or two samples were removed, depending on the signal stability.

a- and b-wave detection

After outlier detection and averaging, a- and b-waves were identified. The a-wave trough was defined as the minimum response between 0 and 30 milliseconds after stimulus onset. The b-wave peak was defined as the maximum response between 15 and 100 milliseconds after stimulus onset. The a-wave *amplitude* was defined as the difference between the baseline and the a-wave trough, whereas the b-wave amplitude was defined as the difference between the b-wave peak and the a-wave trough.

Noise correction

Although sample averaging reduces much of the noise, there will always be some left. The amount of noise has an effect on the minimum and maximum values that are determined: the more noise, the more extreme these values will be. Since we focus on the 'extremes', this effect will be directional and not cancel itself out even when many measures are taken, as is often the case with noise. To control for this, the a-wave trough and b-wave peak were reduced (corrected towards zero) by subtracting a value that was based on the noise level in the baseline period preceding the stimulus.

We did this for a- and b-wave separately. These values were defined as the 5% and 95% (for a- and b-wave respectively) percentile of the difference between individual baseline samples and the baseline average. In fact we calculated these values for the first and second half of the baseline period separately and used the least extreme values. This way (and by ignoring the extreme 5%'s of the noise levels altogether) we reduced the chance of using artifacts or unrepresentative noise values

for the correction. This indeed flattened the amplitudes for animals that were expected not to give any response at all (data not shown).

Curve fitting

We used a modified version of than Naka-Rushton curve to fit a curve through the log(intensity) x b-wave amplitude data. The Naka-Rushton curve is often used in this case because it can nicely fit the saturation. A modification was deemed necessary because most of our results showed super-saturation: the highest response was seen before the highest intensity flash, after that the amplitudes started to decrease again. Fitting was done with matlab® using multidimensional Nelder-Mead minimization. The final curve fit function:

$$f(x) = \frac{rm \times x^n}{b^m + x^m}$$

From the resulting fit functions, two parameters were deduced: *maximum response* and *log-i50*. The first is the maximum amplitude and the second the log10 of the stimulus intensity that resulted in a response 50% of the maximum.

OP analysis

Oscillatory potentials were derived by applying 5th order Butterworth bandpass filter (65-300Hz), as was previously shown to be suitable for mice.[30,31] A one sided frequency spectrum was determined using FFT (Fast Fourier Transform) and the ratio between the power at 75 and 110 Hz was used as a measure for subsequent analysis.

Statistics

The C57Bl/6J mice were compared with the other three groups on various parameters using two-sided *t*-tests (equal variances not assumed). In all cases, the within-mouse average was calculated (from results based on the two protocol runs) before doing the actual tests. Group sizes were 4, 3, 4 and 2 for C57Bl/6J, DBA/2OlaHsd, C3H/HeNHsd and BALB/c respectively for all tests.

Reference List

1. Lumiled V Emitter - Technical Data DS34. www.lumileds.com .

2. Peachey, N. S. & Ball, S. L. Electrophysiological analysis of visual function in mutant mice. *Doc.Ophthalmol.* **107**, 13-36 (2003).

3. Dalke, C. & Graw, J. Mouse mutants as models for congenital retinal disorders. *Exp.Eye Res.* **81**, 503-512 (2005).

4. Paskowitz, D. M., LaVail, M. M., & Duncan, J. L. Light and inherited retinal degeneration. *Br.J.Ophthalmol.* **90**, 1060-1066 (2006).

5. Huttl, S. *et al.* Impaired channel targeting and retinal degeneration in mice lacking the cyclic nucleotide-gated channel subunit CNGB1. *J.Neurosci.* **25**, 130-138 (2005).

6. Wenzel, A. *et al.* RPE65 is essential for the function of cone photoreceptors in NRL-deficient mice. *Invest Ophthalmol.Vis.Sci.* **48**, 534-542 (2007).

7. Masu, M. *et al.* Specific deficit of the ON response in visual transmission by targeted disruption of the mGluR6 gene. *Cell* **80**, 757-765 (1995).

8. Biel, M. *et al.* Selective loss of cone function in mice lacking the cyclic nucleotide-gated channel CNG3. *Proc.Natl.Acad.Sci.U.S.A* **96**, 7553-7557 (1999).

9. Balkema, G. W. Elevated dark-adapted thresholds in albino rodents. *Invest Ophthalmol.Vis.Sci.* **29**, 544-549 (1988).

10. Jablonski, M. M. *et al.* An ENU-induced mutation in Rs1h causes disruption of retinal structure and function. *Mol.Vis.* **11**, 569-581 (2005).

11. Hartong, D. T., Berson, E. L., & Dryja, T. P. Retinitis pigmentosa. *Lancet* **368**, 1795-1809 (2006).

12. Pinto, L. H. & Enroth-Cugell, C. Tests of the mouse visual system. *Mamm.Genome* **11**, 531-536 (2000).

13. Pinto, L. H. *et al.* Results from screening over 9000 mutation-bearing mice for defects in the electroretinogram and appearance of the fundus. *Vision Res.* **44**, 3335-3345 (2004).

14. Dalke, C. *et al.* Electroretinography as a screening method for mutations causing retinal dysfunction in mice. *Invest Ophthalmol.Vis.Sci.* **45**, 601-609 (2004).

15. Niemeyer, G. ERG components of negative polarity from the inner retina and the optic nerve response. *Documenta Ophthalmologica* **111**, 179-189 (2005).

16. Pinto, L. H., Invergo, B., Shimomura, K., Takahashi, J. S., & Troy, J. B. Interpretation of the mouse electroretinogram. *Doc.Ophthalmol.* (2007).

17. Lyubarsky, A. L. & Pugh, E. N., Jr. Recovery phase of the murine rod photoresponse reconstructed from electroretinographic recordings. *J.Neurosci.* **16**, 563-571 (1996).

18. Hagins, W. A., Penn, R. D., & Yoshikami, S. Dark current and photocurrent in retinal rods. *Biophys.J.* **10**, 380-412 (1970).

19. Penn, R. D. & Hagins, W. A. Kinetics of the photocurrent of retinal rods. *Biophys.J.* **12**, 1073-1094 (1972).

20. Tian, N. & Slaughter, M. M. Correlation of dynamic responses in the ON bipolar neuron and the b-wave of the electroretinogram. *Vision Res.* **35**, 1359-1364 (1995).

21. Layton, C. J., Safa, R., & Osborne, N. N. Oscillatory potentials and the b-Wave: Partial masking and interdependence in dark adaptation and diabetes in the rat. *Graefes Arch.Clin.Exp.Ophthalmol.* **245**, 1335-1345 (2007).

22. Wachtmeister, L. Oscillatory potentials in the retina: what do they reveal. *Prog.Retin.Eye Res.* **17**, 485-521 (1998).

23. LASANSKY, A. & DE ROBERTIS, E. Submicroscopic analysis of the genetic distrophy of visual cells in C3H mice. *J.Biophys.Biochem.Cytol.* **7**, 679-684 (1960).

24. Nambu, H., Yuge, K., Shikata, N., Tsubura, A., & Matsuzawa, A. Fas-independent apoptosis of photoreceptor cells in C3H mice. *Exp.Anim* **45**, 309-315 (1996).

25. Gresh, J., Goletz, P. W., Crouch, R. K., & Rohrer, B. Structure-function analysis of rods and cones in juvenile, adult, and aged C57bl/6 and Balb/c mice. *Vis.Neurosci.* **20**, 211-220 (2003).

26. Owen, K., Thiessen, D. D., & Lindzey, G. Acrophobic and photophobic responses associated with the albino locus in mice. *Behav.Genet.* **1**, 249-255 (1970).

27. Schlamp, C. L., Li, Y., Dietz, J. A., Janssen, K. T., & Nickells, R. W. Progressive ganglion cell loss and optic nerve degeneration in DBA/2J mice is variable and asymmetric. *BMC.Neurosci.* **7**, 66 (2006).

28. Janaky, M., Grosz, A., Toth, E., Benedek, K., & Benedek, G. Hypobaric hypoxia reduces the amplitude of oscillatory potentials in the human ERG. *Doc.Ophthalmol.* **114**, 45-51 (2007).

29. Brule, J., Lavoie, M. P., Casanova, C., Lachapelle, P., & Hebert, M. Evidence of a possible impact of the menstrual cycle on the reproducibility of scotopic ERGs in women. *Doc.Ophthalmol.* **114**, 125-134 (2007).

30. Lei, B., Yao, G., Zhang, K., Hofeldt, K. J., & Chang, B. Study of rod- and cone-driven oscillatory potentials in mice. *Invest Ophthalmol.Vis.Sci.* **47**, 2732-2738 (2006).

31. Zhang, K., Yao, G., Gao, Y., Hofeldt, K. J., & Lei, B. Frequency spectrum and amplitude analysis of dark- and light-adapted oscillatory potentials in albino mouse, rat and rabbit. *Doc.Ophthalmol.* **115**, 85-93 (2007).

32. Bayer, A. U. *et al.* Retinal morphology and ERG response in the DBA/2NNia mouse model of angle-closure glaucoma. *Invest Ophthalmol.Vis.Sci.* **42**, 1258-1265 (2001).

33. Porciatti, V., Saleh, M., & Nagaraju, M. The pattern electroretinogram as a tool to monitor progressive retinal ganglion cell dysfunction in the DBA/2J mouse model of glaucoma. *Invest Ophthalmol.Vis.Sci.* **48**, 745-751 (2007).

34. Harlan Netherlands BV. http://www.harlaneurope.com/main_nl.htm .

35. Wong, A. A. & Brown, R. E. Visual detection, pattern discrimination and visual acuity in 14 strains of mice. *Genes Brain Behav.* **5**, 389-403 (2006).

36. Bravo-Nuevo, A., Walsh, N., & Stone, J. Photoreceptor degeneration and loss of retinal function in the C57BL/6-C2J mouse. *Invest Ophthalmol.Vis.Sci.* **45**, 2005-2012 (2004).

37. Lyubarsky, A. L., Falsini, B., Pennesi, M. E., Valentini, P., & Pugh, E. N., Jr. UV- and midwave-sensitive cone-driven retinal responses of the mouse: a possible phenotype for coexpression of cone photopigments. *J.Neurosci.* **19**, 442-455 (1999).

38. Jacobs, G. H. & Williams, G. A. Contributions of the mouse UV photopigment to the ERG and to vision. *Doc.Ophthalmol.* (2007).

39. Jacobs, G. H., Williams, G. A., & Fenwick, J. A. Influence of cone pigment coexpression on spectral sensitivity and color vision in the mouse. *Vision Res.* **44**, 1615-1622 (2004).

40. Neitz, M. & Neitz, J. The uncommon retina of the common house mouse. *Trends Neurosci.* **24**, 248-250 (2001).

41. Gouras, P. & Ekesten, B. Why do mice have ultra-violet vision? *Exp.Eye Res.* **79**, 887-892 (2004).

42. Peachey, N. S., Alexander, K. R., & Fishman, G. A. Visual adaptation and the cone flicker electroretinogram. *Invest Ophthalmol.Vis.Sci.* **32**, 1517-1522 (1991).

43. Alexander, K. R. & Raghuram, A. Effect of contrast on the frequency response of synchronous period doubling. *Vision Res.* **47**, 555-563 (2007).

44. Kondo, M. & Sieving, P. A. Primate photopic sine-wave flicker ERG: vector modeling analysis of component origins using glutamate analogs. *Invest Ophthalmol.Vis.Sci.* **42**, 305-312 (2001).

45. Crevier, D. W. & Meister, M. Synchronous period-doubling in flicker vision of salamander and man. *J.Neurophysiol.* **79**, 1869-1878 (1998).

46. Jacobs, G. H., Neitz, J., & Krogh, K. Electroretinogram flicker photometry and its applications. *J.Opt.Soc.Am.A Opt.Image Sci.Vis.* **13**, 641-648 (1996).

47. Brainard, D. H., Calderone, J. B., Nugent, A. K., & Jacobs, G. H. Flicker ERG responses to stimuli parametrically modulated in color space. *Invest Ophthalmol.Vis.Sci.* **40**, 2840-2847 (1999).

48. Saszik, S. M., Robson, J. G., & Frishman, L. J. The scotopic threshold response of the dark-adapted electroretinogram of the mouse. *J.Physiol* **543**, 899-916 (2002).

49. Li, C., Cheng, M., Yang, H., Peachey, N. S., & Naash, M. I. Age-related changes in the mouse outer retina. *Optom.Vis.Sci.* **78**, 425-430 (2001).

50. Marmor, M. F., Holder, G. E., Seeliger, M. W., & Yamamoto, S. Standard for clinical electroretinography (2004 update). *Doc.Ophthalmol.* **108**, 107-114 (2004).

51. Barnard, A. R., Hattar, S., Hankins, M. W., & Lucas, R. J. Melanopsin regulates visual processing in the mouse retina. *Curr.Biol.* **16**, 389-395 (2006).

52. Mizota, A. & Adachi-Usami, E. Effect of body temperature on electroretinogram of mice. *Invest Ophthalmol.Vis.Sci.* **43**, 3754-3757 (2002).